CHAPTER 4

4-RESULTS

In this chapter it will discuss the results come out from the algorithm developed; in particular those come from smoke detection algorithm and image geo-referencing tool. The system, as mentioned before, is located in Sanremo (IM)-Italy, and it is fixed on Protezione Civile's building roof. The area of monitoring is the Mediterranean-Alpine orography in the West-Liguria near to the France border. The portion monitored is rich of Mediterranean maquis vegetation and rural environment. SIRIO from September 2010 up to December 2011 has collected a big amount of data in the form of visible images came from the Canon Powershot. The system, piloted by VM95, was able to take, compose and send the image from Protezione Civile to Politecnico Server using a simple ADSL connection cable. Just to notice, about 20.000 images are taken and sent during this period and the algorithms has elaborated them in real time provided alarm if necessary. In order to validate we have taken into account smoke and fire generated from farmer burning of vegetation. This procedure, according with the rule of law, is often did by the farmer. In this case, setting the parameters able to detect it, as sensitivity and bins resolution, we can validate the algorithm advantaging from this procedures. SIRIO is fixed as test system and the sensitivity is set according to detect the small fire and smoke. In the future, if SIRIO will installed for real dangerous fire detection, the sensitivity will adapted to this purpose.

SMOKE DETECTION RESULTS

In order to validate the algorithm for smoke detection, we utilized the contingency tables and the Relative Operation Characteristic curve (ROC).

In statistics, a contingency table (also referred to as cross tabulation or cross tab) is a type of table in a matrix format that displays the (multivariate) frequency distribution of the variables. It is often used to record and analyze the relation between two or more categorical variables.

The term contingency table was first used by Karl Pearson in "On the Theory of Contingency and Its Relation to Association and Normal Correlation", part of the Drapers' Company Research Memoirs Biometric Series I published in 1904.

A crucial problem of multivariate statistics is finding (direct-)dependence structure underlying the variables contained in high dimensional contingency tables. If some of the conditional independences are revealed, then even the storage of the data can be done in a smarter way (see Lauritzen (2002)). In order to do this one can use information theory concepts, which gain the information only from the distribution of probability, which can be expressed easily from the contingency table by the relative frequencies.

Let us consider a two-class prediction problem (binary classification), in which the outcomes are labeled either as positive (p) or negative (n) class. There are four possible outcomes from a binary classifier. If the outcome from a prediction is p and the actual value is also p, then it is called a true positive (TP); however if the actual value is n then it is said to be a false positive (FP). Conversely, a true negative (TN) has occurred when both the prediction outcome and the actual value are n, and false negative (FN) is when the prediction outcome is n while the actual value is p.

To get an appropriate example in this problem, consider a test that seeks to determine if the algorithm has detected a smoke from fire. A false positive in this

case occurs when there are smoke positive, but actually does not have the smoke. A false negative, on the other hand, occurs when there are smoke negative, when it actually has detected a smoke.

Let us define an experiment from P positive instances and N negative instances. The four outcomes can be formulated in a 2×2 contingency table or confusion matrix, as follows:

Contingency Tables		**Actual Value**		
		p	**n**	**total**
Prediction Outcome	**p'**	**True Positive**	**False Positive**	**P'**
	n'	**False negative**	**True Negative**	**N'**
	total	**P**	**N**	

Table 12: Contingency Table example

From the contingency table listed in the table 12, it is possible to obtain some indexes useful for understanding the algorithm performances. The table 13 shown the main indexes which are calculated from contingency table results.

TRUE POSITIVE (TP)	Eqv with hits
TRUE NEGATIVE (TN)	Eqv with correct negative
FALSE POSITIVE (FP)	Eqv with false alarm
FALSE NEGATIVE (FN)	Eqv with misses
TRUE POSITIVE RATE (TPR)	TPR = TP / P = TP / (TP + FN)
FALSE POSITIVE RATE (FPR)	FPR = FP / N = FP / (FP + TN)
ACCURACY (ACC)	ACC = (TP + TN) / (P + N)
SPECIFICITY (SPC)	SPC=TN / N =TN / (FP + TN) =1 - FPR
POSITIVE PREDICTIVE VALUE (PPV)	Eqv with precision PPV = TP / (TP + FP)
NEGATIVE PREDICTIVE VALUE (NPV)	NPV = TN / (TN + FN)
FALSE DISCOVERY RATE (FDR)	FDR = FP / (FP +TP)

Table 13: indexes from contingency table

The contingency table can derive several evaluation "metrics". To draw an ROC curve, only the true positive rate (TPR) and false positive rate (FPR) are needed. TPR determines a classifier or a diagnostic test performance on classifying positive instances correctly among all positive samples available during the test. FPR, on the other hand, defines how many incorrect positive results occur among all negative samples available during the test.

A ROC space is defined by FPR and TPR as x and y axes respectively, which depicts relative trade-offs between true positive (benefits) and false positive (costs). Since TPR is equivalent with sensitivity and FPR is equal to 1 − specificity, the ROC

graph is sometimes called the sensitivity vs (1 − specificity) plot. Each prediction result or one instance of a confusion matrix represents one point in the ROC space.

As it is possible to see on figure 46 and 47, the best possible prediction method would yield a point in the upper left corner or coordinate (0,1) of the ROC space, representing 100% sensitivity (no false negatives) and 100% specificity (no false positives). The (0,1) point is also called a perfect classification. A completely random guess would give a point along a diagonal line (the so-called line of no-discrimination) from the left bottom to the top right corners. An intuitive example of random guessing is a decision by flipping coins (head or tail).

The diagonal divides the ROC space. Points above the diagonal represent good classification results, points below the line poor results. Note that the output of a poor predictor could simply be inverted to obtain points above the line.

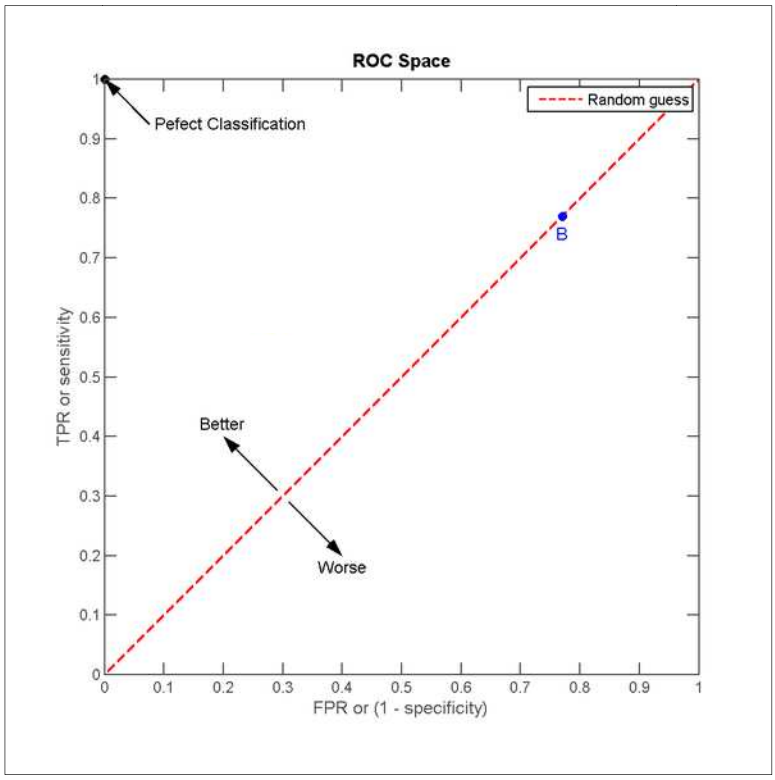

Figure 46: ROC curve.

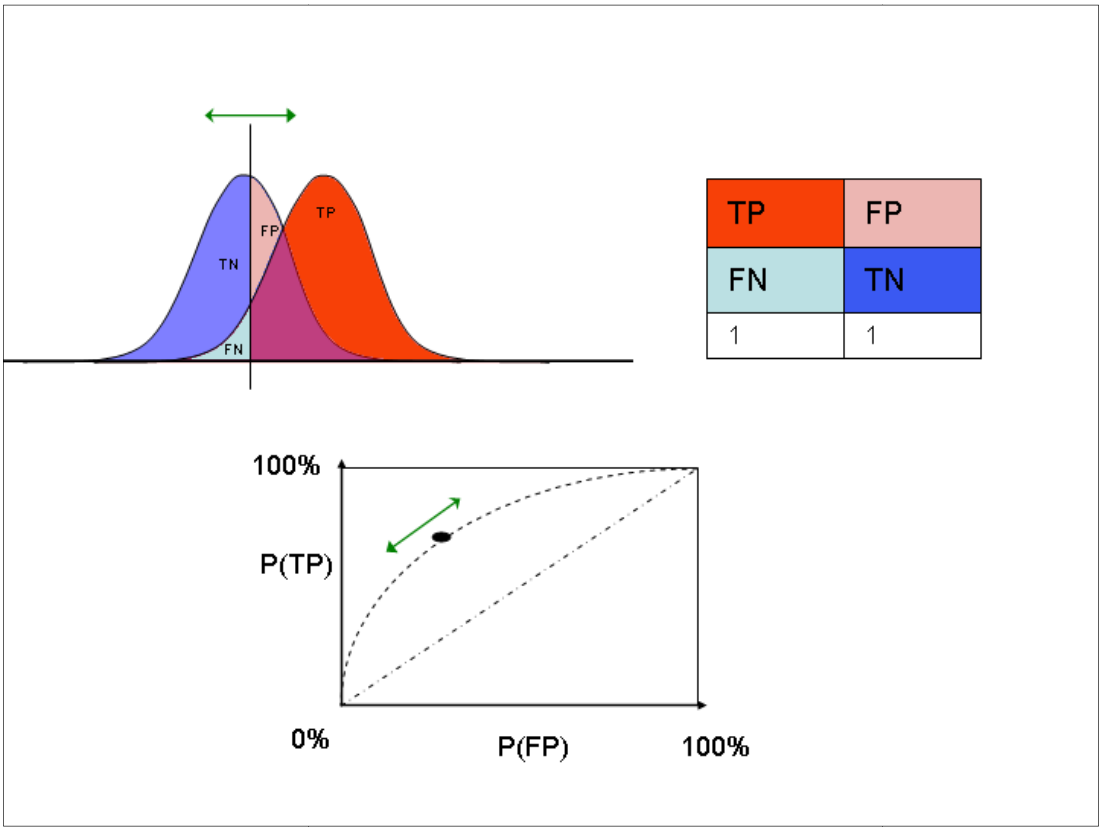

Figure 47: ROC curve

In order to well-understanding the contingency table and ROC curve and in order to adapt to our case, the table and curve can summarized as follows:

	ALARM	NO ALARM
SMOKE	Hits	False Alarm
NO SMOKE	Misses	Correct Negatives

Table 14: Contingency table Smoke detection

The indexes can write in this way as well and the most important are taken into account:

Probably of Detection (POD)	POD = Hits / (Hits + Misses)
Probably Of False Detection (POFD)	POFD = False Alarm / (Correct Neg. + False Alarm)
False Alarm Rate (FAR)	FAR = False Alarm / (Hits + False Alarm)
Accuracy (ACC)	ACC = (Hits + Correct neg.) / total

Table 15: Indexes for Smoke Detection Algorithm

The ROC curve show us a better behaviour when the characteristic curve teds to the top-left, the POD tends to 1 and POFD tends to 0.

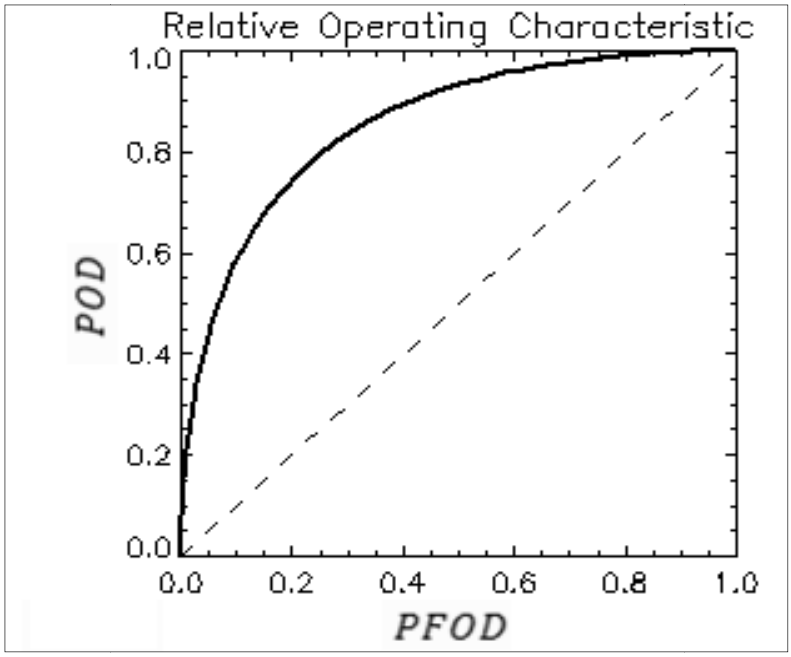

Figure 48: ROC curve example

Since from this brief introduction, the results are summarize in the figure and table below. The images analyzed are taken from 8am to 18pm, depending on the light during the season, they are even selected from almost 20.000 do not including

those of affected by significant mistakes. The mistakes could generated from system malfunction or environmental condition. Form summer 2011, a meteo station was installed, equipping SIRIO system with a rain gauge. The rain gauge provides to stop the smoke detection algorithm when the amount of rain is bigger than a threshold set a priori. In this case a lot of images are cut-off and the images utilized for validation are 12387.

The final purpose is generate the ROC curve, changing the sensitivity *p* (see chapter 3) from a minimum of 10 to 70. The curve will be an important graphical and viewing method to understand the best optimal sensitivity trade-off. The results obtained are shown below on the table 16a,b,c,d

Sensitivity =10	SMOKE	NO SMOKE
ALARM	834	402
NO ALARM	118	11035

(a)

Sensitivity =30	SMOKE	NO SMOKE
ALARM	738	300
NO ALARM	212	11137

(b)

Sensitivity =50	SMOKE	NO SMOKE
ALARM	635	207
NO ALARM	315	11230

(c)

Sensitivity =70	SMOKE	NO SMOKE
ALARM	513	102
NO ALARM	437	11335

(d)

Table 16: (a) Contingency table for p = 10; (b) Contingency table for p = 30; (c) Contingency table for p = 50;(d) Contingency table for p = 70;

The sensitivity changing is done in order to find the optimal threshold to set into the algorithm for the Sanremo monitoring. The sensitivity represents how the the algorithm is sensitive to the B changing between two images, reference and current image. A great sensitivity detects less real alarm and more missed detection but could detect less false alarm as well. A small sensitivity detects more alarm then great sensitivity that could introduce a bigger false alarm rate.

The indexes calculated from the contingency table are shown on table 17.

Sensitivity =10			
POD	**POFD**	**FAR**	**Accuracy**
0.87	**0.035**	**0.32**	**0.96**

(a)

Sensitivity =30			
POD	**POFD**	**FAR**	**Accuracy**
0.78	**0.026**	**0.28**	**0.95**

(b)

Sensitivity =50			
POD	**POFD**	**FAR**	**Accuracy**
0.67	**0.018**	**0.24**	**0.95**

(c)

Sensitivity =70			
POD	**POFD**	**FAR**	**Accuracy**
0.54	**0.009**	**0.16**	**0.95**

(d)

Table 17: (a) indexes results p=10; (b)) indexes results p=30; (c)) indexes results p=50; (d)) indexes results p=70

Using the indexes is not easily understanding what the sensitivity changing is better than others, according to the ROC curve the behaviour is plotted in the figure

below and as mentioned before the best optimal trade-off is when the curve tends to POD = 1 and POFD tends to 0.

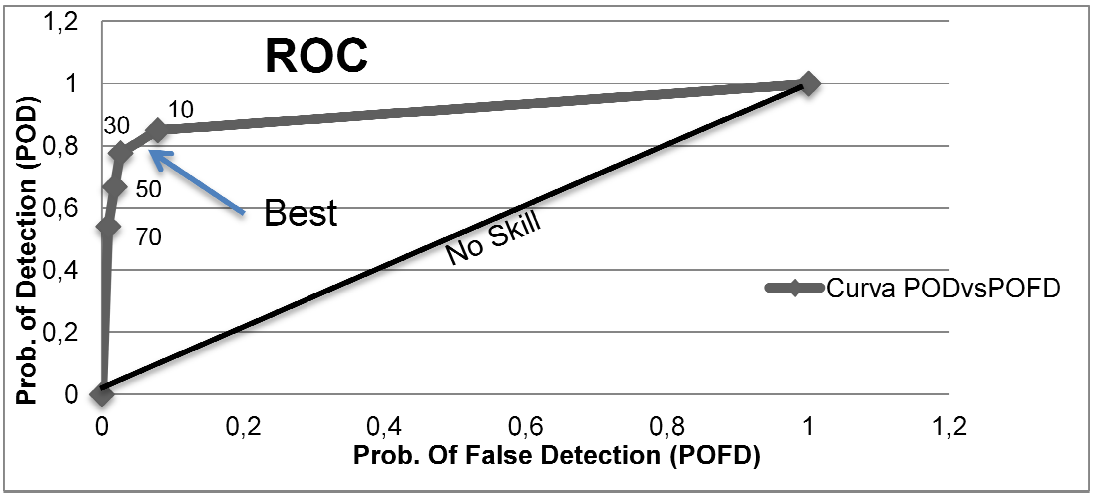

Figure 49: smoke detection results plotted on ROC curve

The figure shows the best value between p = 10 and p = 30, since for the system located in Sanremo the value p = 20 should be the best to set in the Parameter settings. This is just what the results came out, but in term of final settings the sensitivity should be choose according to the operator's needing. For example if the operators want more detection to the detriment of false alarm, they probably should set a value closely to 20. Instead, if they want less false alarm and less detection set a value closely to 30. Our study is just a suggestion instruments to the operator which should choose the value as their own decision.

GEO-REFERENCING RESULTS

As mentioned in the chapter 3, the geo-referencing algorithm generates a geo-refered matrix with dimension NxM, where N are the rows and M are the columns of the image. In order to validate the algorithm it is necessary to measure some point defined as real on the monitored scenario. The real points are taken detecting some visual features into the image. Using a GPS receiver and/or Google Earth application some the real points have been measured and compared with those obtained in the same position on the matrix. For example, a number of 30 measurement for each picture spread in the whole scenario are necessary for calculate the mean error which the algorithm has introduced. Considering the figures below as the real points taken into account on the monitored scenario.

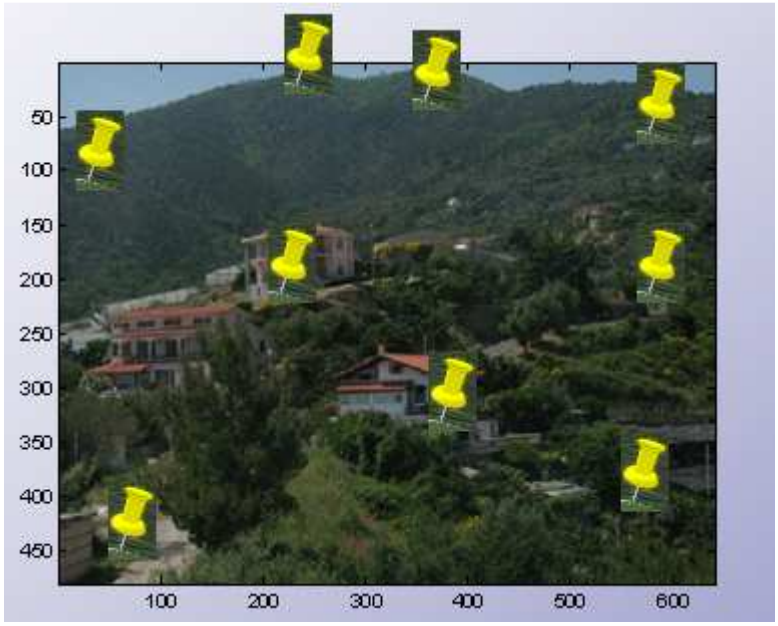

Figure 50: Point of interest on the scenario

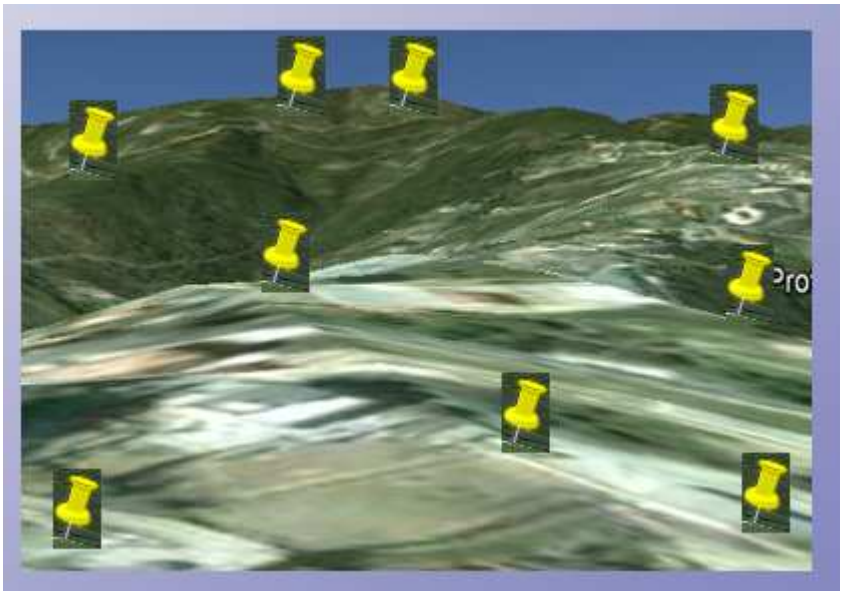

Figure 51: Point of interest on the Google Earth

This point are taken in proximity of visual features on the scene; using GPS or Google Earth (see figure 51) we measure the latitude and longitude for each point and considering the Matrix it is calculated the differences, in the same visual point, between real point (measured with GPS and Google Earth) and matrix point (calculated with the algorithm). It is also analyzed the differences in term of meters and plotted into a graph trough a histogram.

Since to the deep of images, it is important to note that the pixel have different size and area between foreground and background pixel. This is possible because the matrix is obtained using projective and geometric transformation of image trough a DEM (see chapter 3). Therefore, the differences between real and calculated point may not be the same behaviour at every distance. For this reason, a validation threshold has been introduced. The validation is done using threshold at 1.5km and 2km from the camera location.

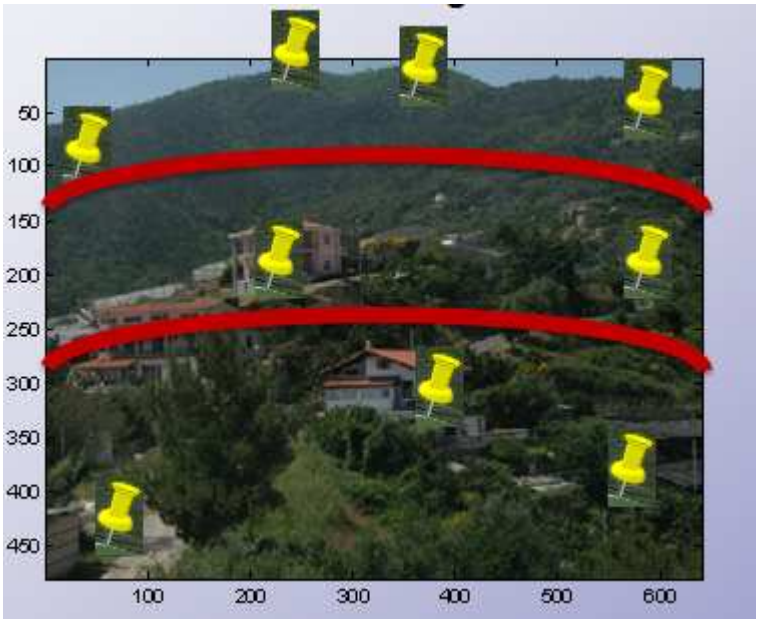

Figure 52: Point of interest on the scenario with threshold

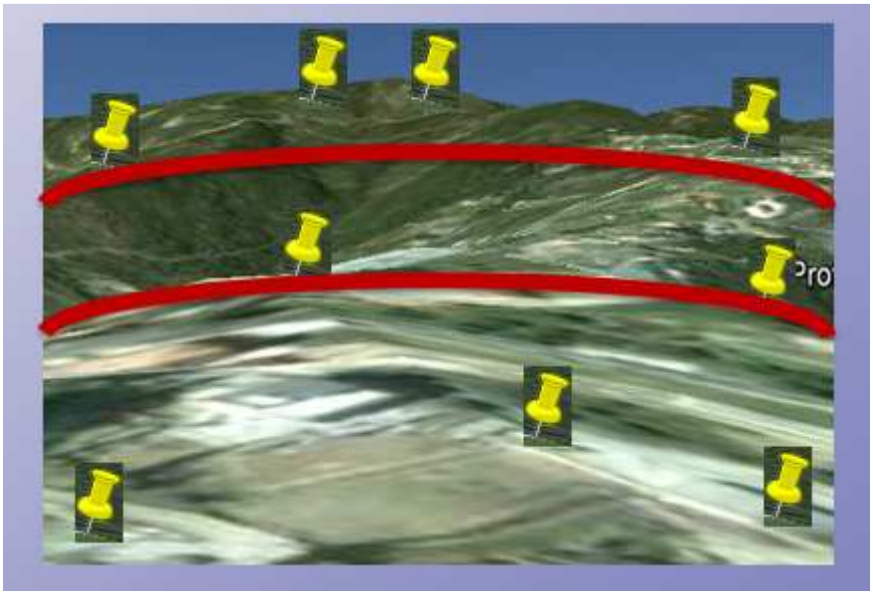

Figure 52: Point of interest on Google Earth with threshold

In order to obtain that results some important indexes has been calculated: Mode, Median, Mean and Standard Deviation defined in [20]. Before of that, let us define the statistical indexes.

MODE

In statistics, the *mode* is the value that occurs most frequently in a data set or a probability distribution. In some fields, notably education, sample data are often called scores, and the sample mode is known as the modal score.

Like the statistical mean and the median, the mode is a way of capturing important information about a random variable or a population in a single quantity. The mode is in general different from the mean and median, and may be very different for strongly skewed distributions.

The *mode* is not necessarily unique, since the same maximum frequency may be attained at different values. The most ambiguous case occurs in uniform distributions, wherein all values are equally likely.

MEAN

For a data set, the mean is the sum of the values divided by the number of values. The mean of a set of numbers x1, x2, ..., xn is typically denoted by $\bar{x}$, pronounced "x bar". This mean is a type of arithmetic mean. If the data set were based on a series of observations obtained by sampling a statistical population, this mean is termed the "sample mean" ($\bar{x}$) to distinguish it from the "population mean" (μ or μx). The mean is often quoted along with the standard deviation: the mean describes the central location of the data, and the standard deviation describes the spread. An alternative measure of dispersion is the mean deviation, equivalent to the average absolute deviation from the mean. It is less sensitive to outliers, but less mathematically tractable.

The arithmetic mean is the "standard" average, often simply called the "mean".

$$\bar{x} = \frac{1}{n} \cdot \sum_{i=1}^{n} x_i \qquad (4.3)$$

MEDIAN

In probability theory and statistics, median is described as the numerical value separating the higher half of a sample, a population, or a probability distribution, from the lower half. The median of a finite list of numbers can be found by arranging all the observations from lowest value to highest value and picking the middle one. If there is an even number of observations, then there is no single middle value; the median is then usually defined to be the mean of the two middle values.

In a sample of data, or a finite population, there may be no member of the sample whose value is identical to the median (in the case of an even sample size), and, if there is such a member, there may be more than one so that the median may not uniquely identify a sample member. Nonetheless, the value of the median is uniquely determined with the usual definition.

STANDARD DEVIATION

Standard deviation is a widely used measure of variability or diversity used in statistics and probability theory. It shows how much variation or "dispersion" exists from the average (mean, or expected value). A low standard deviation indicates that the data points tend to be very close to the mean, whereas high standard deviation indicates that the data points are spread out over a large range of values.

The standard deviation of a random variable, statistical population, data set, or probability distribution is the square root of its variance. It is algebraically simpler though practically less robust than the average absolute deviation. A useful property of standard deviation is that, unlike variance, it is expressed in the same units as the data. The standard deviation, typically represents as σ (sigma), contain 68% of measure while the reported margin of error is typically about twice the standard

deviation , the radius of a 95% confidence interval. Let X be a random variable with mean value μ:

$$\mathrm{E}[X] = \mu. \tag{4.2}$$

Here the operator E denotes the average or expected value of X. Then the standard deviation of X is the quantity

$$\sigma = \sqrt{\mathrm{E}[(X - \mu)^2]}. \tag{4.3}$$

An example of Mean, Mode, Median and Standard Deviation are represent on figure 53a and 53b.

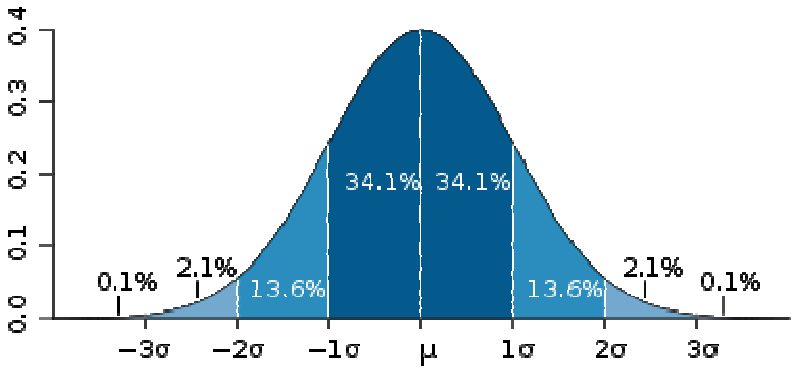

Figure 53a: Example Standard Deviation (Normal distribution)

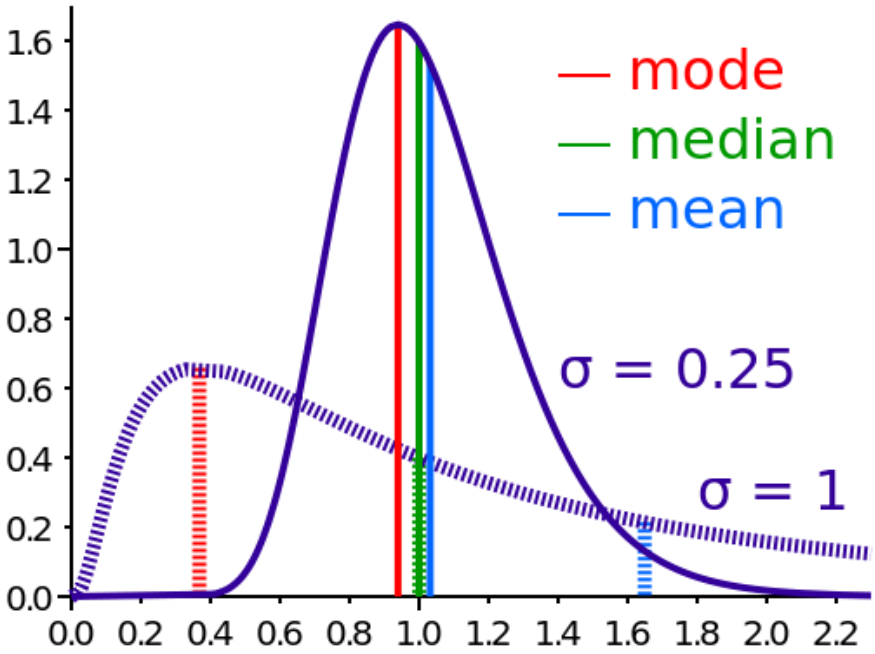

Figure 53b: Example of Mode, Mean and Median on Gaussian Distribution

First of all, the validation and the histogram of geo-referencing tool, are obtained without considering the threshold and the result are shown on figures below and the indexes are listed on table 18-19-20-21-22-23.

Results

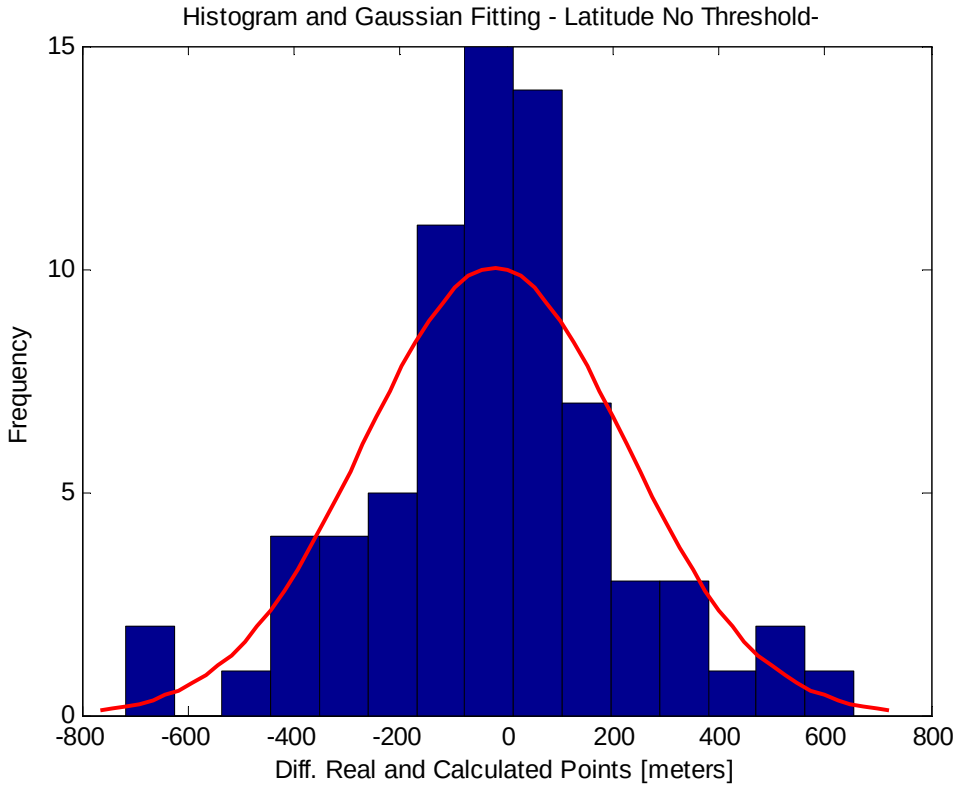

Figure 54: Histogram and Gaussian Fitting for Latitude using all Points

LATITUDE [meters] NO THRESHOLD			
Mode	**Median**	**Mean**	**Standard Deviation**
-30	**-12**	**-21.4**	**248**

Table 18: indexed of Mode, Median, Mean and Standard Deviation related to Latitude without threshold

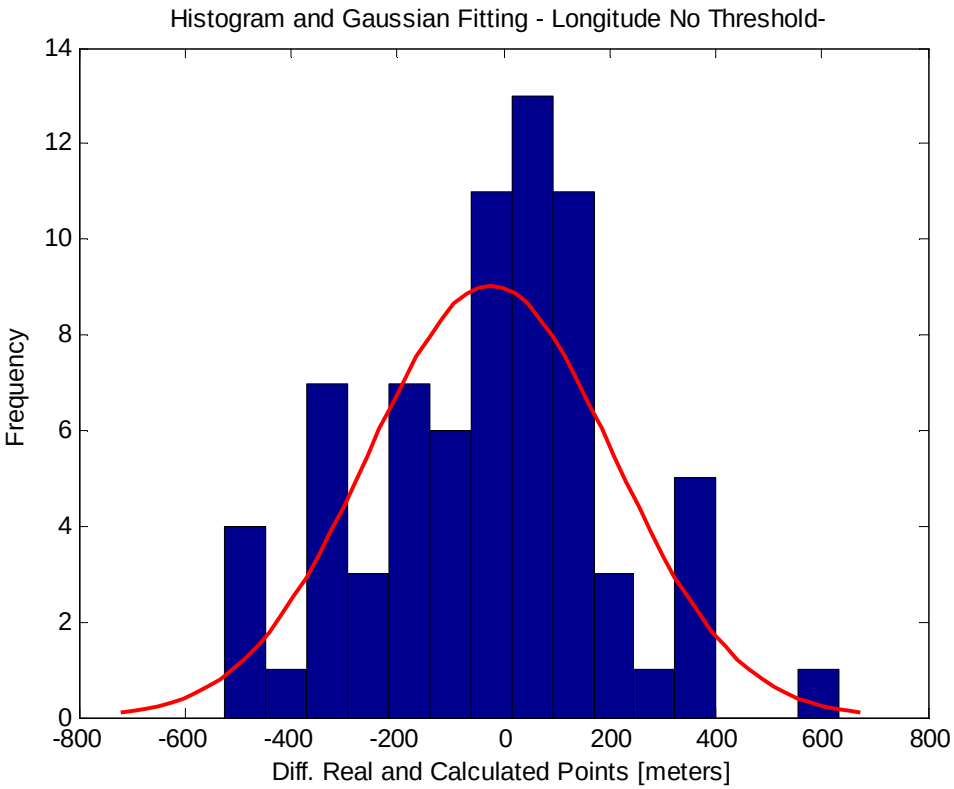

Figure 55: Histogram and Gaussian Fitting for Longitude using all Points

LONGITUDE [meters] NO THRESHOLD			
Mode	**Median**	**Mean**	**Standard Deviation**
40	**4**	**-23.59**	**231**

Table 19: indexed of Mode, Median, Mean and Standard Deviation related to Longitude without threshold

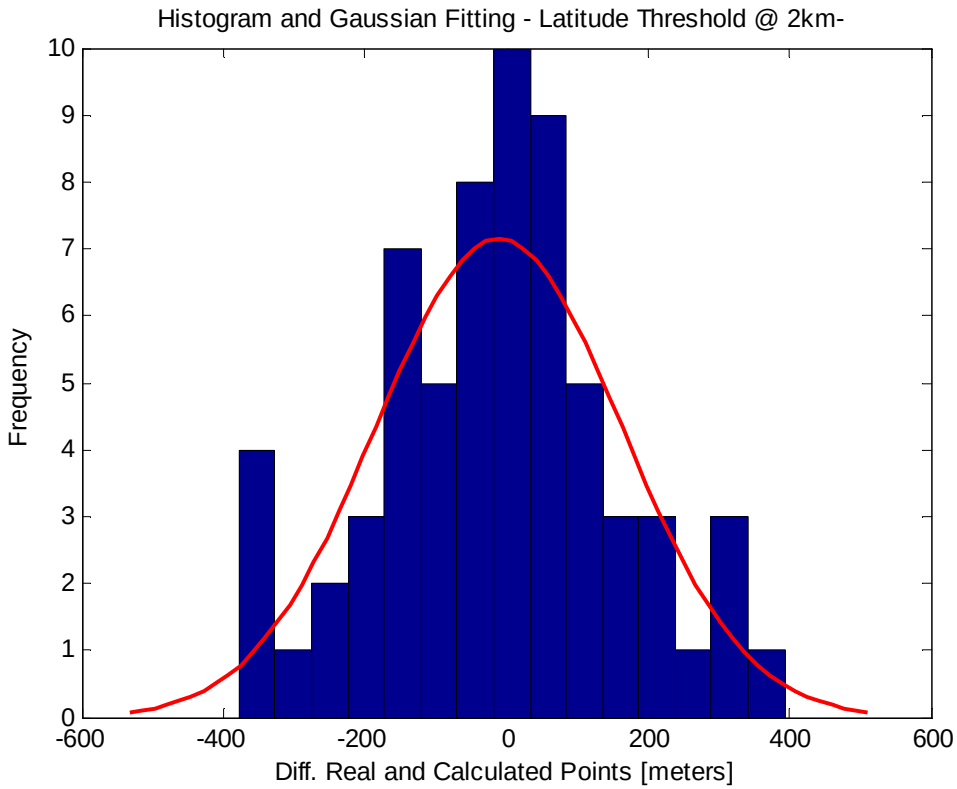

Figure 56: Histogram and Gaussian Fitting for Latitude using Threshold @ 2km

LATITUDE [meters] THRESHOLD@2km			
Mode	**Median**	**Mean**	**Standard Deviation**
10	**-12**	**-10**	**173**

Table 20: indexed of Mode, Median, Mean and Standard Deviation related to Latitude with threshold @ 2km

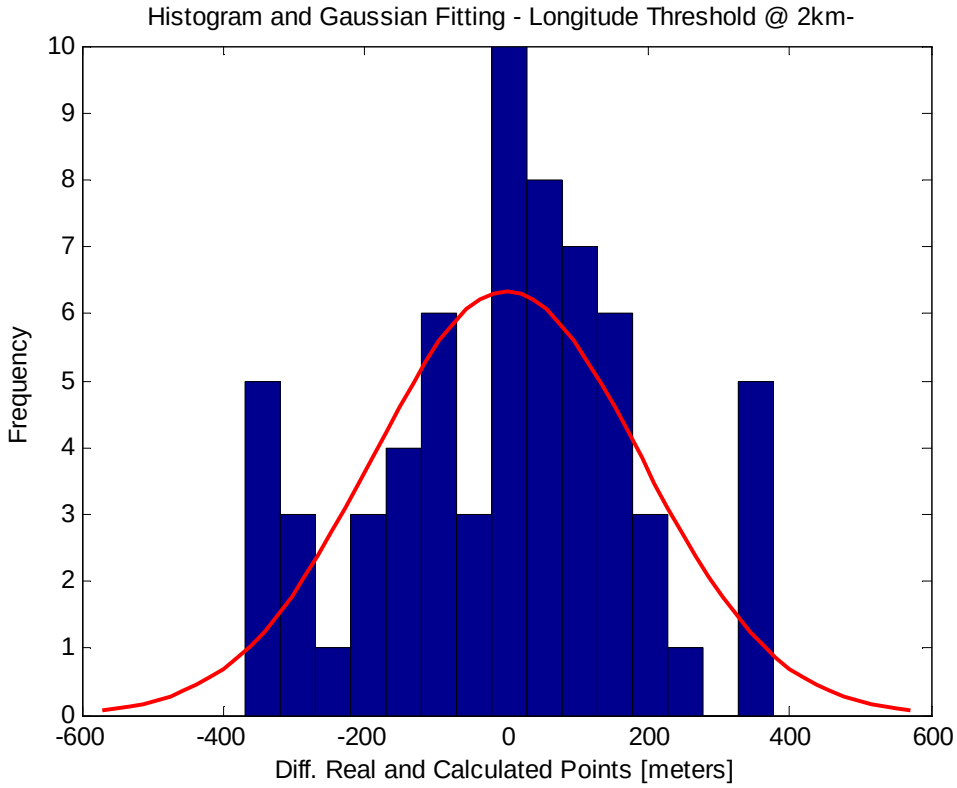

Figure 57: Histogram and Gaussian Fitting for Longitude using Threshold @ 2km

LONGITUDE [meters] THRESHOLD@2km			
Mode	**Median**	**Mean**	**Standard Deviation**
0	**-12**	**0.6**	**190**

Table 21: indexed of Mode, Median, Mean and Standard Deviation related to Longitude with threshold @ 2km

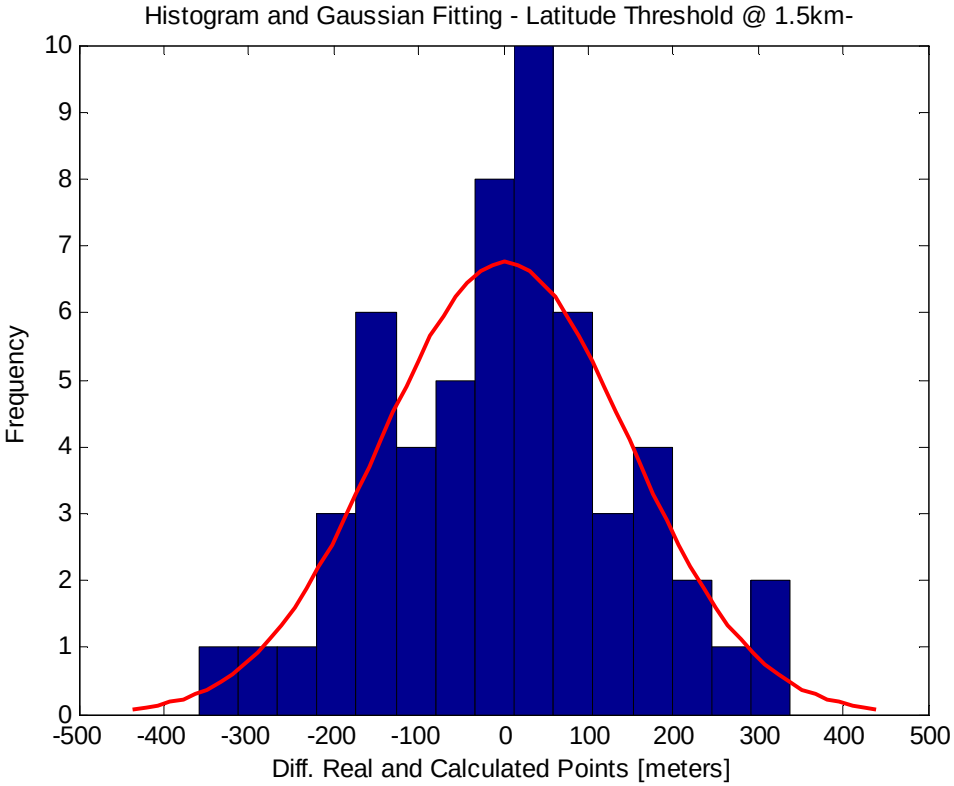

Figure 58: Histogram and Gaussian Fitting for Latitude using Threshold @ 1.5km

LATITUDE [meters] THRESHOLD@1.5km			
Mode	**Median**	**Mean**	**Standard Deviation**
35	**4**	**2**	**145**

Table 22: indexed of Mode, Median, Mean and Standard Deviation related to Latitude with threshold @ 1.5km

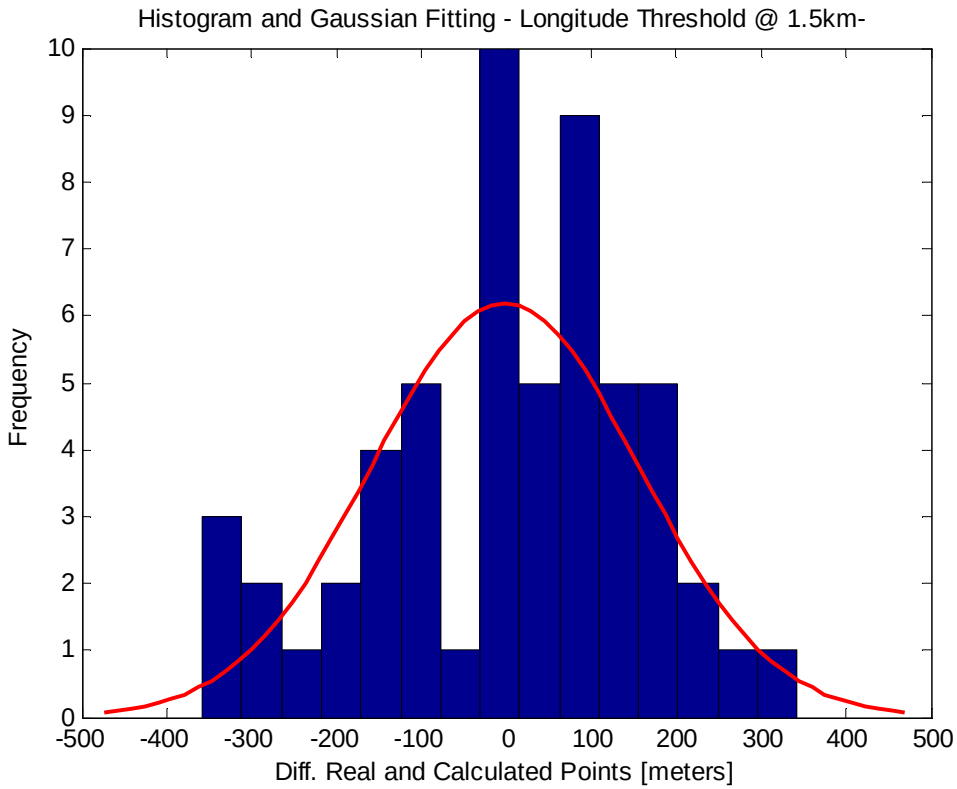

Figure 59: Histogram and Gaussian Fitting for Longitude using Threshold @ 1.5km

LONGITUDE [meters] THRESHOLD@1.5km			
Mode	**Median**	**Mean**	**Standard Deviation**
0	**7**	**-1.4**	**150**

Table 23: indexed of Mode, Median, Mean and Standard Deviation related to Longitude with threshold @ 1.5km

The figures shown that using different threshold the results going to be better behaviour because the pixel closer to the sensor are less subject to have errors as mentioned before. The index which is able to show the behaviour is the Standard Deviation, remember that it is the value within are concentrated the 68% of the measures. From table 18 and 19 the standard deviation is quite high, respective 248m Latitude and 231m Longitude. Considering a DEM with100m of resolution, without threshold, the error could be approximately two and half DEM pixel.

If we consider a threshold at 2km from the sensors, the value of Standard Deviation is going to be better than without threshold in both case, latitude and longitude. The table 20 and 21 show us a Standard deviation equal to 173m and 190m and also from the figures 56 and 57 is possible to see the tail disappearing respect to the figures 54 and 55.

The last threshold is set at 1.5km, and also in this case we obtain a better behaviour respect to the previous threshold. As a matter of fact, the index which show the behaviour, the Standard Deviation, is: 145m for the latitude and 150m for the longitude, that means an error in the order of one DEM pixel.

The figures show us an Histogram related to the frequency of the error introduced. The error is the difference between the real point measured by GPS or Google Earth and the calculated point found by the geo-referencing algorithm. The Gaussian in red, is a fitting curve of histogram and show a qualitative behaviour of the result, in this case the error.

CHAPTER 5

5-DECISION SUPPORT AND USER INTERFACE

As shown in the figure 2, the final step of our forest fires system is the user layer, that is the final product user oriented developed according to the operators mandatory. That means, SIRIO system is tailored for every situation and operations as the orography, the environment, the position and the sensitivity order to set.

A Graphic User Interface (GUI) was developed in order to help the operator and to give an early warning message, as e-mail or SMS, in case the algorithms detect a fire severity. In case of fire, a decision support tool show on a Google maps the fire position and the support layers position as well.

The support layers position as: Water Point supply, Helicopter Landing, Road, Access Way and Squad locations are very useful for the operators because it provides to know the initial plan strategy to adopt for the forest fires extinguish. Before that it is necessary to know for every layers, the latitude and longitude position and this is possible only through an initial calibration phase using knowing geographical layers location.

The GUI, through a decision support algorithm, show to the operator which layers are closer to the event of fire and give a geographical positions on the Google map as well as the fire latitude and longitude. The figure 60a show the example of GUI utilized by operator.

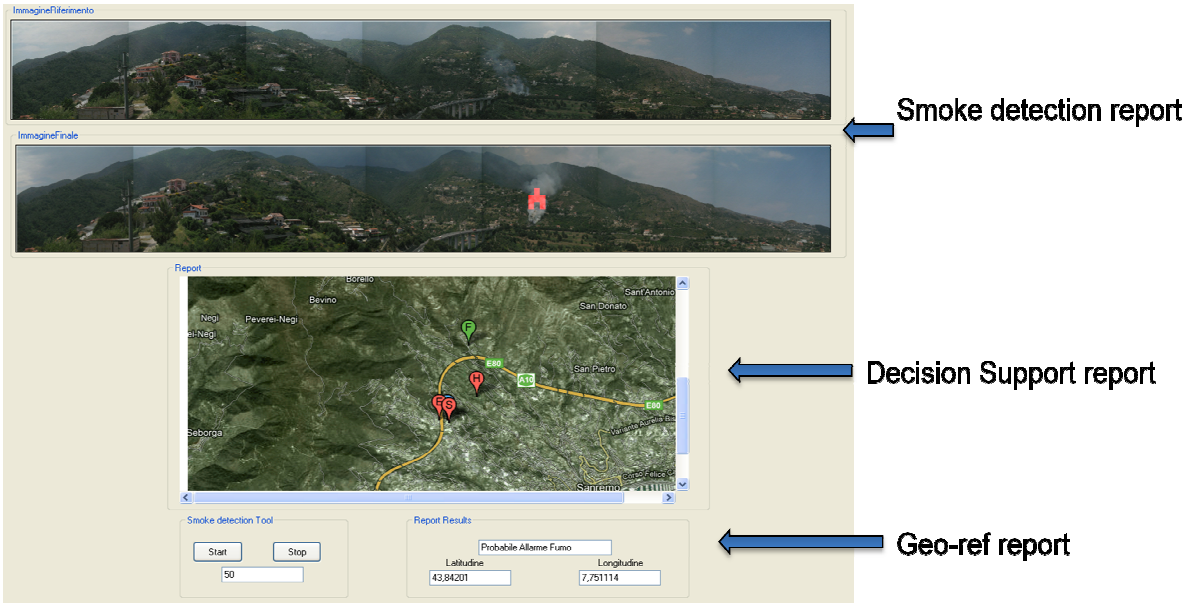

Figure 60a: example of GUI with Smoke detection report, Decision Support report and Geo-referencing report.

Figure 60b: Smoke detection report

Figure 60c: Decision Support report

Figure 60d: Geo-referencing report

Figure 60b visualizes the images that come from the smoke detection algorithm with, if recognized, the smoke pattern. At this point an alarm is sent to the operator which they can analyze the images and decide if it is correct detection or false alarm. At the mean time automatically, the Decision Support algorithm, gives the fire position as well as the support layers (see figure 60c). From that figure it is possible to see the layers automatically placed into the map in the correct geographic location. The label F is the position of the Fire, H is the Water point supply, S is the Squad location and E is the Helicopter landing. From this Google Map is easily to see and understand the road and access way to the fire severity.

Figure 60d show the Geo-referencing Report, with a Report result and fire latitude and longitude position in degree. For example this forest fires has 43,84° Latitude and 7,75° Longitude. This event was a real forest fires detected by SIRIO on 25th May 2011 at 2.00 p.m.

In order to give a further help to operator, a Web Page was developed, it is shown on figure 61.

Figure 61a: Web Page of SIRIO system

From this Web Page it is possible to see the immediately alarm signaling report as Alarm or Situation OK. Even, it is possible to interact with the button for visualize the real situation and the images that are used from the smoke detection algorithm (see figure 61b).

As well as the smoke detection, there are other features which could used by people from the Web page. *"DATI METEO"* concerned the whole environmental data taken from the rain gauge installed with the SIRIO system (see figure 61c). That is useful because stops the forest fires algorithms when rains.

"Hot Spot Detection" button, as Smoke detection provides to show the thermal images in real time. The last button, *"Immagini Live"*, show the data base where the last 700 images are stored (see figure 61d). This is useful in order to check the history and helps the operator in the decision support as well. The Web Page is automatically refreshed every 3 minutes.

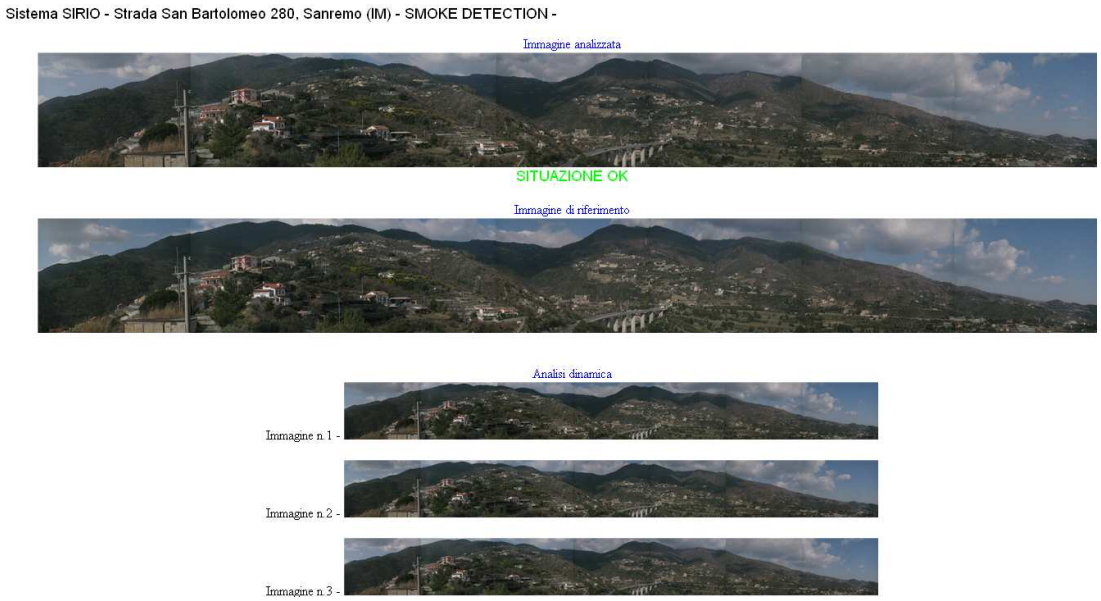

Figure 61b: Smoke Detection button

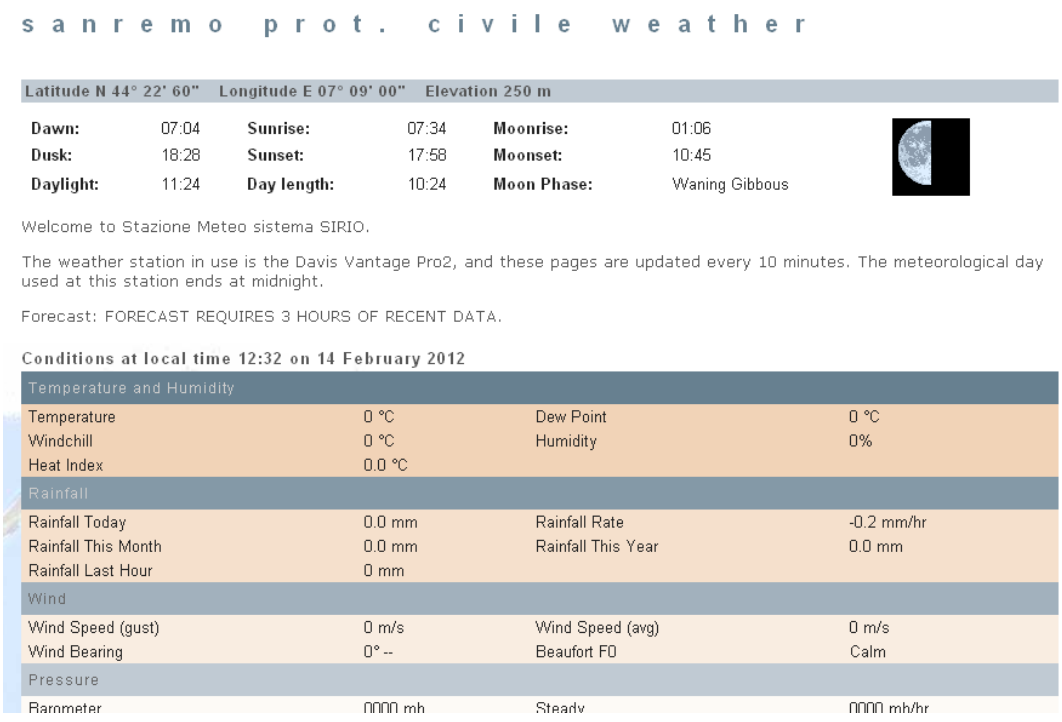

s a n r e m o p r o t . c i v i l e w e a t h e r

Latitude N 44° 22' 60" Longitude E 07° 09' 00" Elevation 250 m

Dawn:	07:04	**Sunrise:**	07:34	**Moonrise:**	01:06
Dusk:	18:28	**Sunset:**	17:58	**Moonset:**	10:45
Daylight:	11:24	**Day length:**	10:24	**Moon Phase:**	Waning Gibbous

Welcome to Stazione Meteo sistema SIRIO.

The weather station in use is the Davis Vantage Pro2, and these pages are updated every 10 minutes. The meteorological day used at this station ends at midnight.

Forecast: FORECAST REQUIRES 3 HOURS OF RECENT DATA.

Conditions at local time 12:32 on 14 February 2012

Temperature and Humidity			
Temperature	0 °C	Dew Point	0 °C
Windchill	0 °C	Humidity	0%
Heat Index	0.0 °C		
Rainfall			
Rainfall Today	0.0 mm	Rainfall Rate	-0.2 mm/hr
Rainfall This Month	0.0 mm	Rainfall This Year	0.0 mm
Rainfall Last Hour	0 mm		
Wind			
Wind Speed (gust)	0 m/s	Wind Speed (avg)	0 m/s
Wind Bearing	0° --	Beaufort F0	Calm
Pressure			
Barometer	0000 mb	Steady	0000 mb/hr

Figure 61c: Environmental data from rain gauge

Figure 61d: Live images

Using the GUI and the Web Page, the user terminals can also access the central server for the evaluation of statistical analysis of data stored in the database, for manual control and survey operations and for calibration and diagnostics operations.

This tools user oriented, are useful when, for example, a forest fire squad come from neighbored city for helping the local squad in case of big fire severity. In this case could append that the squad from other city does not know the conformation of orography and consequently the access way or road to operate for fire extinguish are unknown as well.

This system and the algorithms are thought for giving a common plan of strategy in the case mentioned before, the order from a control and operation room will managed by operator and shared with the whole squad forces easily as early as possible using the GUI and Web Page developed.

CHAPTER 6

6-CONCLUSIONS AND FUTURE WORKS

SIRIO integrated system has been tested over different monitoring sessions and test areas and it's now operative in Liguria for wildfire monitoring and early warning. SIRIO achieves high performances in reliability, robustness flexibility, cost and consumption. From September 2010 up to now it provides a great reliability to the environmental condition for every season (Autumn, Winter, Spring and Summer).

It continued to work very well under summer sun and autumn rains and wind. SIRIO shows us a great flexibility due to modular architecture, the system is able to work with the whole sensors and algorithms or using one algorithm and sensor at time. This allows, to the operators, to use it setting the system according to the boundary conditions as: weather, orography, land cover, season etc. Even, the modular architecture provides reliability in term of power consumption and cost.

The price of the system is directly dependent to how many commercial sensors and algorithms are equipped and developed for the system. For this reasons, the system is low-cost oriented suited for complex orography and for every land cover condition.

It guarantees accurate hot spot and smoke identification and produces geo-referenced information sets very useful for an effective decision support activities.

Just for resume the results, smoke detection algorithm has an accuracy (Hits + Correct Negative) equal to 96% and in the georef. tool results, the standard deviation show us an error in the order of one DEM pixel. The system has also enhanced territory monitoring and intervention planning for the operators.

The Remote Sensing Group of Politecnico di Torino, is under continuous development: at present a new false alarm reduction tool based on combined VIS/NIR images is in the process of being implemented. Near Infrared images (NIR)

are using for a new develop study, an implementation of new algorithm able to reduce the false alarm which the other algorithms, especially hot-spot algorithm, could introduce. The process implemented is also a modular algorithm which can used or not depending on the operators whishes.

The main idea for the future is to develop more algorithms which run independently from each other, giving a certain freedom degree in correlation with the cost and performance trade-off.

Concerning our results we can say that in order to reduce smoke detection error and false alarm rate, a frequency combination of images (NIR, TIR and VIS) could reduce the indexes POFD and FAR. That means a combinations of more sensors as the system has been thought and equipped.

In order to improve the geo-referencing performance a more detailed DEM is needed. In our results we are working with a DEM, download by free, with a spatial resolution in the order of 100 meters. Since the geo-referencing algorithm works with geometric and projective transformation of DEM (see chapter 3), there is a directly dependence between DEM resolution and the precision of geographic pixel found by algorithm. As much as the DEM resolution is high, a better result, in term of precision, is found but the cost could increase.

In our case, using a DEM with 100 meters of resolution, we have obtained an error around 150 meters in both of geographical coordinates.

Anyway, this results, for our applications is a good compromise between cost and performance.

The system equipped with the commercial sensor could be used for other environmental monitoring applications. SIRIO was designed against the deforestation caused by forest fires and suited algorithms are been developed for this purpose.

Since the sensors are sensed from visible to NIR domain, see table 5, algorithms for environmental hazard which are sensed as well to the SIRIO frequency domain, could be implemented and developed.

For that reason, a study of volcanoes monitoring hazard has been done and it will discuss in the Appendix chapter. The studying is done during the European exchange program between Remote Sensing Group of Polytechnic Turin and the Wessex Institute of Technology of Southampton, UK.

REFERENCES FOR SIRIO SYSTEM

[1] Ricerca Forestale, www.ricercaforestale.it.

[2] Osservatorio Incendi boschivi, www.incendiboschivi.org

[3] Mazzeo, G.; Marchese, F.; Filizzola, C.; Pergola, N.; Tramutoli, V.; *A Multi-temporal Robust Satellite Technique (RST) for Forest Fire Detection, Analysis of Multi-temporal Remote Sensing Images*, 2007. MultiTemp 2007. International Workshop

[4] Casbeer, D.W.; Beard, R.W.; McLain, T.W.; Sai-Ming Li; Mehra, R.K, *Forest fire monitoring with multiple small UAVs*, American Control Conference, 2005. Proceedings of the 2005

[5] Martinez-de Dios, J.R.; Ollero, A.; *Wavelet applications to forest-fire monitoring and measurement, Automation* Congress, 2002 Proceedings of the 5th Biannual World , 2002

[6] Zhong Zhang Jianhui Zhao Dengyi Zhang Chengzhang Qu Youwang Ke Bo Cai, *Contour Based Forest Fire Detection Using FFT and Wavelet*, Wuhan, Hubei , dec. 2008

[7] Liyang Yu; Neng Wang; Xiaoqiao Meng; *Real-time forest fire detection with wireless sensor networks, Wireless Communications, Networking and Mobile Computing*, 2005. Proceedings. 2005 International Conference

[8] Fernández-Berni, J., Carmona-Galán, R., Carranza-González, L., *A vision-based monitoring system for very early automatic detection of forest fires*, Institute of Microelectronics of Seville - Centro Nacional de Microelectrónica Consejo Superior de Investigaciones Científicas y Universidad de Sevilla, 2008.

[9] Archetti R., Torricelli E., Erdman R., Lamberti A., *first application of a new imaging system for the coastal monitoring*, Bologna

[10] R. Archetti e A. Lamberti., *studio dell'evoluzione di una spiaggia protetta da opera a cresta bassa mediante videomonitoraggio*

[11] Corgnati L., Gabella M., Perona G., FIREcast system - Previsional fire danger index computation system for alpine regions. *1st International Conference on Forest Fires 2008, 17-19 September 2008, Toledo (Spain).*

[12] Viney, N.R., Hatton, T., Modelling the effect of condensation on moisture content of forest litter., *Agricultural and Forest Meteorology* 51, 1990.

[13] Simard, A.J., The moisture content of forest fuels. A review of the basic concepts, *Canadian Department of Forest and Rural Development, Forest Fire Research Institute, Ottawa, Ontario*, Information Report FF-X-14, 1968.

[14] Van Wagner, C.E., Pickett, T.L., Equations and FORTRAN program for the Canadian Forest Fire Weather Index System, *Canadian Forestry Service, Petewawa Forest Experimental Station, Chalk River, Ontario*, Technical Report 33, 1985.

[15] Viney, N.R., Catchpole, E.A., Estimating fuel moisture response times from field observations, *International Journal of Wildland Fire*, 1991.

[16] Rothermel, R.C., Wilson, R., Morris, G., Sackett, S., Modelling moisture content of fine dead wildland fuels: input to the BEHAVE fire prediction system., *United States Department of Agriculture, Forest Service, Intermountain Research Station Ogden, Utah*, Research Paper INT-359, 1986

[17] Nelson, R.M, A method for describing equilibrium moisture content of forest fuels, *Canadian Journal of Forest Research* 14, 1984.

[18] Van Wagner, C.E, Development and structure of the Canadian forest fire weather index system., *Canadian Forestry Service, Petewawa Forest Experimental Station, Chalk River,Ontario*, Technical Report 35, 1987

[19] A. Losso, L. Corgnati, G. Perona, Innovative *image geo-referencing tool for decision support in wildfires fight*, Forest Fires II international Conference, Kos, Greece, 2010.

[20] Wikipedia web site. Definition of Mode, Median, Mean and Standard Deviation